

# One-dimensional turbulence (ODT): computationally efficient modeling and simulation of turbulent flows

Victoria B. Stephens, David O. Lignell\*

*Chemical Engineering Department, Brigham Young University, Provo, UT 84602, USA*

---

## Abstract

Write this last. About 100 words.

*Keywords:* turbulence, reacting flows, one-dimensional turbulence

---

## Code Metadata

Nr.	Code metadata description	Please fill in this column
C1	Current code version	1.0
C2	Permanent link to code/repository used for this code version	<i>github.com/BYUignite/ODT</i>
C3	Code Ocean compute capsule	N/A
C4	Legal Code License	MIT
C5	Code versioning system used	Git
C6	Software code languages, tools, and services used	C++, Python 3.x, Yaml,
C7	Compilation requirements, operating environments & dependencies	CMake 3.12+, Cantera, Git, Doxygen (optional)
C8	If available Link to developer documentation/manual	N/A
C9	Support email for questions	davidlignellbyu.edu

Table 1: Code metadata (mandatory)

## 1. Motivation and significance

Turbulent flows characterize the vast majority of fluid flows in practical engineering applications, and simulations of turbulent flows provide re-

---

\*Corresponding author.

*Email address:* davidlignell@byu.edu (David O. Lignell)

4 searchers with valuable insights into complex systems, particularly reacting  
5 turbulent flows such as combustion processes. Turbulence is a complex phe-  
6 nomenon that affects the full range of a flow’s length and time scales. As a  
7 result, resolving the entire flow field by numerically solving the Navier-Stokes  
8 equations of fluid flow, as is done in direct numerical simulations (DNS), re-  
9 quires substantial computational resources. DNS is a powerful research tool,  
10 but its high computational cost makes it intractable for simulating most  
11 practical engineering flows. In order to achieve numerical solutions to prac-  
12 tical flow problems, researchers can use alternative frameworks that model  
13 turbulence rather than resolving it directly.

14 Large-eddy simulations (LES) address the problem of wide-ranging length  
15 and time scales by combining direct resolution of grid-scale quantities, as in  
16 DNS, with subgrid modeling of smaller turbulence structures. The more  
17 complex the flow, the more modeling is required; for example, a jet flame  
18 simulation might require subgrid modeling for the combustion chemistry, ra-  
19 diative heat transfer, or soot chemistry in addition to turbulence structures,  
20 all of which form a tightly coupled system in which each model interacts  
21 heavily with the others. While subgrid modeling makes LES more computa-  
22 tionally affordable than DNS, it can introduce empiricism into simulations,  
23 which can lead to inaccurate results. Additionally, unresolved quantities are  
24 often parameterized in state space with empirical relationships or assumed  
25 distributions that lack universal applicability. LES is a valuable simulation  
26 tool, but its approach to turbulence modeling can introduce unwanted em-  
27 piricism and make errors difficult to isolate and quantify.

28 The one-dimensional turbulence model (ODT) functionally reverses the  
29 LES approach, modeling large-scale turbulent advection and directly resolv-  
30 ing small-scale flow structures, simulating the full range of length and time  
31 scales in a single dimension. Because large-scale structures are much easier  
32 to study and model than small-scale structures, ODT mitigates or sidesteps  
33 many of the subgrid modeling issues that complicate LES. Previous stud-  
34 ies show that ODT can attain accuracy comparable to DNS at a fraction  
35 of the computational cost [1, 2], making it an attractive tool for simulating  
36 turbulent flows. Because the ODT model is one-dimensional, it is limited to  
37 homogeneous or boundary-layer flows, such as jets, wakes, and mixing layers;  
38 these types of flows, however, are common in nature and central to turbu-  
39 lence research. ODT’s computational efficiency and resolution of a full range  
40 of scales make it a valuable tool that complements experimental studies and  
41 other simulation tools like DNS and LES.

42 Early applications of ODT focused on homogenous turbulence, wakes, and  
43 mixing layers [3, 4, 5]. Later extension to variable-density flows and a spatial  
44 downstream coordinate system facilitated its growth and application to more

complex flows, including combustion in jet flames [6, 7, 8, 9, 10, 11, 12, 13], counterflow flames [14], wall fires [15], and sooting flames [1, 16, 17, 18, 19], as well as other particle flows [20, 21, 22, 23]. ODT has also served to complement LES through subgrid modeling studies [24, 25, 26] and has been applied to various other flow configurations such as double-diffusive interfaces [27], Rayleigh-Taylor mixing [28], and stratified turbulence [29]. Most recently, the ODT code was extended to include cylindrical and spherical coordinate systems [30, 31, 32].

During the recent implementation of the cylindrical and spherical model formulations, the ODT code was drastically overhauled and reorganized, resulting in its current configuration. The ODT code presented here is a pared down version of the development code, representing the fundamental aspects of the ODT model and its most reliable functions. The example cases in Section 3 are a representative sample of the ODT code’s capabilities as it is presented here. Future releases will expand this code’s functionality with additional features currently in development.

## 2. Software description

### 2.1. Model description

The ODT model is described in detail in the literature [3, 5, 33, 30, 34]; only a brief explanation will be given here. In ODT, turbulent advection is modeled with stochastic processes called eddy events, which punctuate the solution of unsteady, one-dimensional transport equations for mass, momentum, and enthalpy. The ODT code uses a Lagrangian finite-volume formulation for diffusive advancement in which mass stays constant within each grid cell while cell volumes increase or decrease according to cell dilation via an adaptive mesh refinement [34].

Transport equations for mass, momentum, and enthalpy in the temporal formulation of ODT take the following generic form, derived from the Reynolds Transport Theorem [35] for a given scalar quantity per unit mass  $\beta$ :

$$\frac{d\beta}{dt} = -\frac{j_{\beta,e}A_{x,e} - j_{\beta,w}A_{x,w}}{\rho V} + \frac{S_{\beta}}{\rho V}. \quad (1)$$

Here,  $j_{\beta}$  is the diffusion flux of scalar  $\beta$  across the cell face area  $A_x$  where the subscripts  $e$  and  $w$  refer to the "east" and "west" faces of the grid cell, respectively.  $S_{\beta}$  is the Lagrangian source term derived from the conservation law for  $\beta$ ,  $\rho$  represents mass density, and  $V$  represents cell volume. In practice, we refer to the left hand term on the right side of Equation 1 as the "mixing term" and the right hand term on the right side of Equation 1 as the "source term". The generic transport equation differs slightly in the spatial

82 formulation of ODT, but its form is the same, so we omit it here for brevity.  
 83 The system of ordinary differential equations (ODEs) that results is well be-  
 84 haved at all grid points and in all geometries in their finite-volume forms.  
 85 For details on transport equation derivation and use in both the temporal  
 86 and spatial formulations of ODT, see Lignell et al. [30].

87 Eddy events occur as a Poisson process in accordance with their eddy  
 88 rates, where a given eddy event of size  $l$  and location  $x_0$  has an eddy timescale  
 89  $t$  and an associated eddy rate  $1/t$ . Three user-defined ODT parameters  
 90 control the eddy event process: the eddy rate parameter  $C$  scales the rate of  
 91 occurrence of the eddies; the viscous penalty parameter  $Z$  suppresses small  
 92 eddies; and the large eddy suppression parameter  $\beta$  constrains eddies such  
 93 that they do not reach over the elapsed simulation time. Sampled eddies  
 94 that do not fit the defined parameters are rejected and not applied to the  
 95 domain.

96 Eddy events modify domain variables using triplet maps, as illustrated  
 97 for a cylindrical domain in Figure 1. For a region of eddy size  $l$ , the do-  
 98 main is copied to create three map images; the three images are then placed  
 99 back to back with the middle image inverted to maintain continuity, and  
 100 the composite is reapplied to the domain. This process applies to all trans-  
 101 ported variables on the domain. Applied properly, the triplet map increases  
 102 scalar gradients and decreases length scales consistent with the application  
 103 of turbulent eddies in real flows, conserves all quantities and their statistical  
 104 moments, and maintains continuity in property profiles. Subsequent eddies  
 105 in the same region will result in a cascade of scales, and eddy rates depend  
 106 on eddy size and the local kinetic energy such that they follow turbulent  
 107 cascade scaling laws.

108 Eddy events occur concurrently with diffusive advancement via solution  
 109 of the system of unsteady one-dimensional transport equations. In this way,  
 110 the ODT code marches in time or space until it reaches its end point. Due to  
 111 the stochastic nature of eddy events, each ODT simulation, or realization, is  
 112 different, even when it is provided with the same input parameters. In order  
 113 to obtain statistically stable data for a given set of parameters, we run many  
 114 realizations with the same input parameters and time-average them. This is  
 115 done via post-processing tools, which are provided in the ODT package.

## 116 2.2. *Software Architecture*

117 The ODT package consists primarily of an object-oriented C++ code re-  
 118 sponsible for running flow simulation cases and generating data. The package  
 119 also contains auxiliary data processing and visualization tools, written mostly  
 120 in Python. The post-processing tools are case-specific but will be addressed  
 121 generally in Section 2.3.

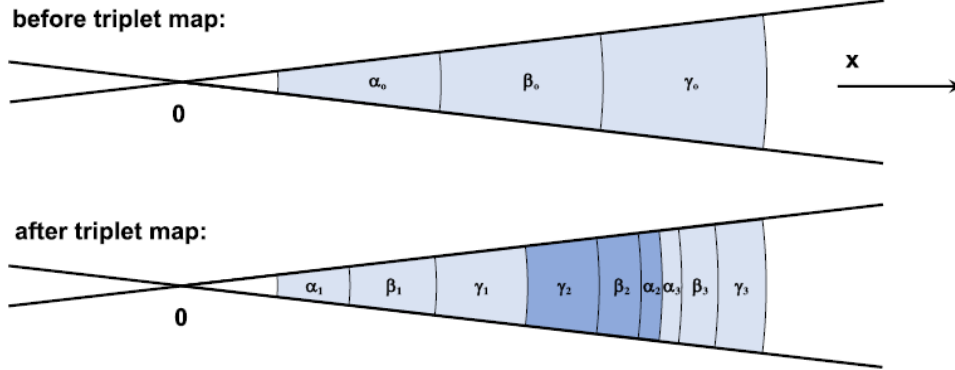


Figure 1: Schematic diagram of a cylindrical triplet map, adapted from [30]. Before the triplet map, the domain contains three grid cells of equal volume, while after the triplet map has been applied, the domain contains nine cells. The nine final cells are labeled according to the cells from which they originated and shaded to indicate that three map images were combined to create the final composite.

Figure 2 illustrates the ODT code’s most important objects and structural features. User inputs are provided to the executable in YAML [36] format via `input.yaml`; the location of the specific `input.yaml` file to be used is determined by the case name and case type specified in the run script. The `main` function defines storage for the main objects, but, once created, the `domain` object is responsible for object initialization as well as variable initialization and storage via a case-specific `domaincase` object.

Three primary objects handle the code’s main functions: the `solver`, `micromixer`, and `eddy` objects. The `solver` coordinates the ODT solution process, marching along the simulation time and invoking diffusive advancement and eddy events when appropriate. The `micromixer` handles diffusive advancement by setting step sizes, interacting with the transported domain variables, and solving the system of ODEs defined by Equation 1 (or its equivalent in the spatial formulation). The `micromixer` includes three solution methods that can be specified in `input.yaml`, each appropriate for various case types: a first-order explicit Euler method (pictured in Figure 2); a first-order semi-implicit method that uses CVODE [37] to advance coupled ODEs in individual grid cells, integrated sequentially; and a second-order Strang splitting method [38] good for treating stiff chemistry. In reacting flow cases, chemical kinetics are handled by Cantera [39], which uses transported variable values—enthalpy and gas species composition, for instance—to specify local scalar values such as gas temperature or density, which can affect flow properties. The `micromixer` is also the code’s primary point of in-

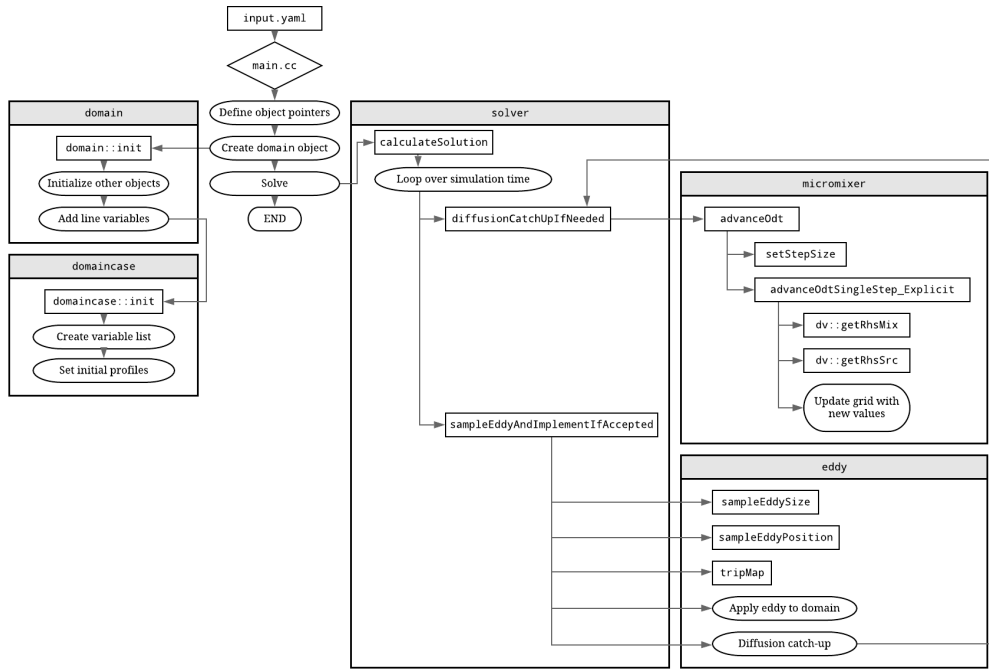


Figure 2: Structural outline of the ODT code, including its major class objects. For brevity, this diagram makes two simplifications. First, it assumes that diffusive advancement in the `micromixer` uses an explicit solution method; in practice, users specify either an explicit, semi-implicit, or Strang split method. Second, it implies that all of the eddy events sampled by the `eddy` object are applied to the domain; in reality, eddy events are filtered through several rejection tests (omitted from this figure for clarity) before acceptance and application to the domain.

145 teraction with the `mesher` object (not pictured in Figure 2), which manages  
146 the adaptive grid functions. Finally, the `eddy` object manages eddy event  
147 selection and implementation, which proceeds as described in Section 2.1.

### 148 2.3. Workflow

149 This section outlines the process a user goes through in order to success-  
150 fully build the ODT code and run a simulation. For more details, please see  
151 the package documentation. ODT is a standalone, self-contained package,  
152 and users interact with its files primarily via the command line rather than  
153 a graphical interface.

154 Within the main download package, several directories organize the ODT  
155 code. The `source`, `build`, and `run` directories contain the ODT source code,  
156 compilation tools, and run scripts, respectively. The `input` directory contains  
157 subdirectories corresponding to several possible case types, each populated  
158 with an appropriate input files. The `data` directory, initially empty, holds  
159 the raw data files and runtime information generated by ODT, as well as  
160 post-processed data files generated from within the `post` directory. Finally,  
161 the `doc` directory contains documentation optionally generated by Doxygen  
162 [40] during the build process.

#### 163 2.3.1. Building ODT

164 The ODT build process is automated with CMake. First, the user nav-  
165 igates to the `build` directory and edits the CMake configuration file. The  
166 CMake configuration file specifies Cantera’s location and must be changed  
167 to reflect the local installation location. Note that the user must also specify  
168 which chemical mechanism the code will compile with. In order to run sim-  
169 ulations with different chemical mechanisms, the code must be recompiled,  
170 including the CMake configuration files, between simulations, whereas this  
171 is not required when other variables are changed. This is a known inconsis-  
172 tency that we plan to address in future code releases. Once the configuration  
173 settings are updated, the user runs CMake to apply the changes.

174 YAML is required in order to process input files. If it has not yet been  
175 installed, it must be built and installed at this point. For convenience, the  
176 ODT package automates this process. YAML need only be installed once  
177 for a given instance of the ODT package. Rebuilding the ODT code with  
178 CMake does not affect the YAML installation.

179 Once CMake and YAML have been prepared, the user can build the ODT  
180 code with the `make` command. There is no associated `install` command that  
181 needs to be run after the `make` command. The most common errors that occur  
182 during the build process concern incorrect file paths or incomplete installation  
183 of required packages. See the build documentation for troubleshooting help.

184 Once the code is built, the user may optionally build a local copy of the  
185 documentation via Doxygen, which must be previously installed. This step is  
186 not required in order to run the ODT code. As an alternative, documentation  
187 can be accessed via `README` files within the code or at the code repository  
188 wiki.

### 189 2.3.2. *Input files*

190 User-modified input files are located within the `input` directory, which  
191 contains subdirectories that correspond to various case types that can be run  
192 with ODT. At minimum, a case's subdirectory must contain an `input.yaml`  
193 file, but may contain other files or subfolders with supplementary informa-  
194 tion.

195 The `input` directory also contains the `gas_mechanisms` subdirectory, which  
196 contains chemical mechanism files that can be used in reacting flow cases.  
197 For cases in which a chemical mechanism is not required, the `not_used.xml`  
198 mechanism file is specified in `input.yaml`. Note that the chemical mech-  
199 anism chosen for the case and specified in the input file must match the  
200 mechanism specified in the CMake configuration file during the ODT build  
201 process.

202 Input files contain simulation parameters in a human-readable format  
203 parsed by YAML. Not all of the parameters in an input file may be used  
204 in a given simulation. Within `input.yaml`, parameters are organized into  
205 sections, several of which are common to all input files. Details about in-  
206 dividual parameters, including usage and typical values, are covered in the  
207 documentation. Prior to running a simulation, users must select and modify  
208 the appropriate `input.yaml` file to reflect the desired simulation conditions.  
209 The default values present in the input files represent general parameters  
210 that may be used to run a successful simulation of that case type.

### 211 2.3.3. *Running ODT*

212 To run a simulation, users must then navigate to the `run` directory, which  
213 contains the `odt.x` executable and several possible run scripts. The simplest  
214 option is `runOneRlz.sh`, which runs one realization of ODT in the specified  
215 configuration. In this run script, the user must alter two variables near the  
216 top of the file: `inputDir`, which specifies which input directory and files to  
217 use; and `caseName`, which provides a name for the simulation and the data  
218 files it outputs. The `runManyRlz.sh` script runs many realizations in serial,  
219 one after the other; it differs from `runOneRlz.sh` only in that the user must  
220 also alter the `nRlz` variable, which specifies the number of realizations to  
221 run. To run the simulation with either `runOneRlz.sh` or `runManyRlz.sh`,  
222 save the run script and execute it at the command line. Users will see some



223 output on the command line, but no data, which is instead output to the  
224 **data** directory.

225 ODT simulations can also be run in parallel using MPI. Two run scripts,  
226 **slrmJob.sh** and **slrmJob\_array.sh**, are configured using SLURM [41], a  
227 common workload manager used for massively parallel computing resources.  
228 This allows many ODT realizations to run in parallel rather than in serial,  
229 reducing overall simulation time. Individual realizations are independent  
230 and do not affect one another, but users must take care with case names and  
231 input file changes to ensure that individual realizations or entire cases are  
232 not overridden accidentally.

#### 233 2.3.4. *Data files and post-processing*

234 For a given simulation, data is output to the **data** directory, which con-  
235 tains subdirectories for each simulation, specified by the **caseName** variable  
236 in the run script. Figure 3 illustrates the structure of the **data** directory and  
237 the locations of files within it. Each case folder is subdivided into **input**,  
238 **runtime**, **data**, and **post**. The **input** folder contains a copy of the input  
239 files used for the simulation, **runtime** contains runtime output information,  
240 **data** contains the raw data files, and **post** contains post-processed data files  
241 once they are generated.

242 To use post-processing tools, navigate to the **post** directory. Within the  
243 **post** directory, data processing tools are organized by case type, which is  
244 specified in **input.yaml** and determines case-specific variables and simula-  
245 tion setup parameters (refer to the **domaincase** object in Figure 2). Each  
246 set of post-processing tools is different, but may contain some combina-  
247 tion of Python scripts (often coordinated by a **driver.py** file), experimental  
248 data files for comparison and plot generation, or other supplementary files.  
249 Post-processed data and generated plots are deposited in the **data** directory,  
250 within the appropriate **caseName/post** folder. For more information on using  
251 the provided post-processing tools, please refer to the documentation.

### 252 3. Example Case: Canonical Jet Flame

253 ODT is uniquely suited for reacting flow simulations. Here, we present  
254 illustrative ODT simulation results of a round, turbulent jet flame based on  
255 and compared to the experimental DLR-A flame of Meier et al. [42]. This  
256 canonical flame configuration has been used extensively to study and validate  
257 turbulent combustion models [43, 44, 45, 46, 47, 48].

258 The DLR-A fuel stream is mixture of 22.1% CH<sub>4</sub>, 33.2% H<sub>2</sub>, and 44.7%  
259 N<sub>2</sub> (by volume) that issues into dry air via a nozzle with an inner diameter  
260 of 8 mm at a mean exit velocity of 42.2 m·s<sup>-1</sup>. The coflow air stream issues

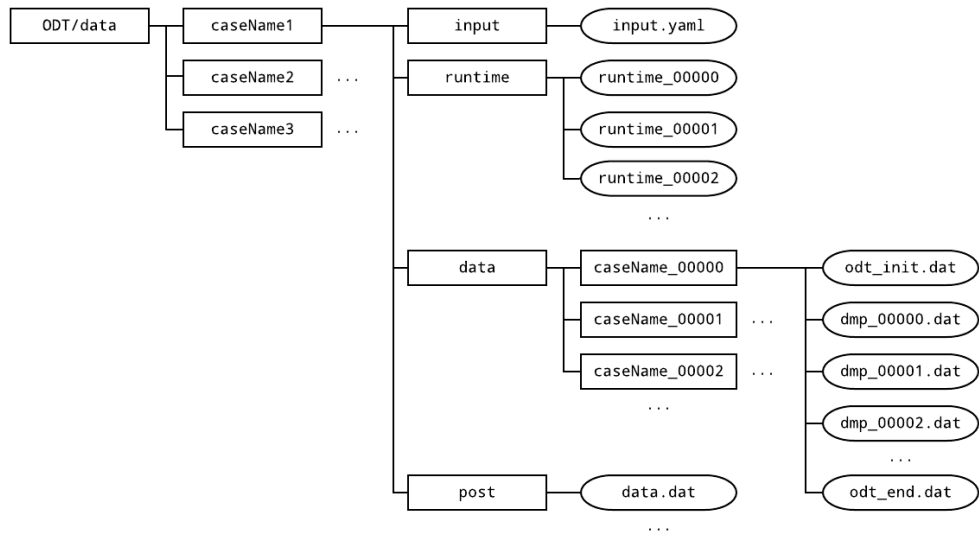
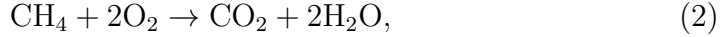


Figure 3: Data folder structure and file locations. Boxes indicate folders and ovals indicate files. For a given simulation, **caseName** will be replaced with the case name specified in the run script. The number attached to **caseName** folder names and to **runtime** data files indicates the realization number. The number attached to **dmp** files indicates the output time step, or "dump" time, of the data file. These correspond to the order of the time steps listed in **input.yaml**.

261 from a concentric nozzle 140 mm in diameter at a velocity of  $0.3 \text{ m}\cdot\text{s}^{-1}$ . The  
 262 reported jet Reynolds number is 15,200.

Previous ODT studies of turbulent jet flames have used the temporal planar formulation, but the spatial cylindrical formulation developed recently [30] more closely matches the experimental configuration. This simulation uses the experimentally reported velocity profiles and jet dimensions. The fuel was diluted with  $\text{N}_2$  in the experimental flame to minimize radiative heat losses, and radiation is ignored in the simulation. This flame has a low Reynolds number, and the combustion chemistry proceeds quickly. The ODT simulation transports the chemical species  $\text{O}_2$ ,  $\text{N}_2$ ,  $\text{CH}_4$ ,  $\text{H}_2$ ,  $\text{H}_2\text{O}$ , and  $\text{CO}_2$ . We assume that reactions proceed to the products of complete combustion and apply simple, fast reaction rates according to the following chemical equations:



263 These assumptions are not reasonable for the DLR-A flame, but they allow us  
 264 to illustrate ODT in a reacting jet configuration with variable properties and  
 265 heat release. More complex combustion reaction mechanisms are available  
 266 within the source code and can be accessed by changing the appropriate  
 267 input file parameters.

268 This simulation uses ODT parameters  $C = 20$ ,  $\beta_{LES} = 17$ , and  $Z = 400$ .  
 269 The values of  $C$  and  $\beta_{LES}$  were adjusted to give good agreement with the  
 270 experimental data, and the value of  $Z$  is the same as the spatial simulations  
 271 in [15]. 1024 independent flow realizations were performed in parallel and  
 272 the results ensemble averaged. Downstream distance  $y$  and radial position  $r$   
 273 are normalized by the jet diameter  $D$ .

274 Figure 3 displays the simulation results: axial mean and centerline values  
 275 for (a) axial velocity  $v$ , (b) mixture fraction  $\xi$ , and (c) temperature  $T$ . The  
 276 ODT results track the experimental data well for all three variables. The  
 277 centerline temperature peaks about 100 K above the experimental data, but  
 278 this small difference can be attributed to thermal radiation (which was ne-  
 279 glected in this simulation) and the assumption that reactions proceed to the  
 280 products of complete combustion rather than their equilibrium state. The  
 281 centerline velocity shows a fast initial decrease that can be attributed to dif-  
 282 fusion. Similarly, the increase in centerline velocity RMS values is delayed;  
 283 this occurs due to the elapsed time model for large eddy suppression, which  
 284 limits disturbances in the early stages of the flow to small eddies that occur  
 285 on the jet edges away from the centerline.

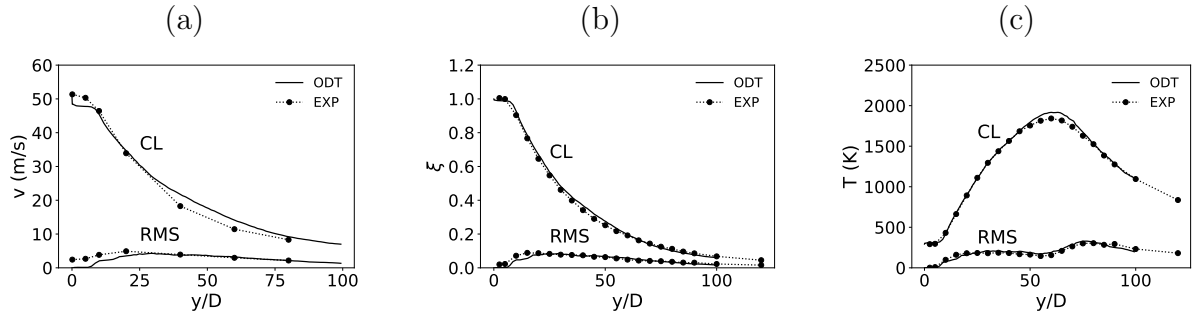


Figure 4: DLR jet flame example case results: (a) mean axial velocity and RMS velocity along the centerline versus downstream location; (b) mean axial mixture fraction and RMS mixture fraction along the centerline versus downstream location; (c) mean axial temperature (K) and RMS temperature (K) along the centerline versus downstream location.

286 To replicate this example case, build the code with the `CHEMISTRY =`  
 287 `SIMPLEDLR` flag in the `user_config` file and edit the desired run script with  
 288 `inputDir = "../input/jetFlame/DLR_A"` and a new case name such as  
 289 `caseName = "jetFlame_example"`. The input file for this case, located at  
 290 `ODT/input/jetFlame/DLR_A/input.yaml`, already contains the appropriate  
 291 parameters and does not need to be modified to match this example case.  
 292 Please see the code documentation for data post-processing instructions.

## 293 4. Impact

294 Questions to answer in this section (from SoftwareX template)

- 295 1. How can new research questions be pursued with this software?
- 296 • possibility of parametric studies (much harder with DNS/LES/RANS)
  - 297 • study of late-flame soot and radiation interactions, soot emissions
  - 298 as smoke
  - 299 • comparative radiation model studies?
- 300 2. How does the software improve pursuit of existing research questions?
- 301 • late-flame behavior becomes easier to study
  - 302 • validation of LES subgrid models
  - 303 • soot stuff, especially late in the flame (because soot moves slowly
  - 304 compared to gas species and therefore short simulation times like
  - 305 in DNS aren't enough to study it effectively)
- 306 3. How does the software change the daily practice of its users?

- 307           • cases take hours or days rather than weeks using supercomputer  
308           resources
- 309           • test cases can be run on local computers (unlike something like  
310           DNS) and as background tasks without disrupting other tasks
- 311           • ODT as a tool complements other approaches, can cover blind  
312           spots and be used in validation
- 313   4. How widespread is the software? Who uses it? (Within and outside of  
314   intended research area and/or group.)
- 315           • BYU group
- 316           • JCH at Sandia
- 317           • Chalmers group in Sweden (Marco Fistler, etc.)
- 318           • German university group (Heiko Schmidt, Juan Media, Marten  
319           Klein, etc.)
- 320           • TO DO: find other groups who have used or currently use ODT
- 321   5. How is the software used in commercial settings (if any)? Has it led to  
322   creation of spin-off companies?
- 323           • No commercial use (I think).

## 324   **5. Conclusion**

325   Write this part next to last

## 326   **6. Conflict of Interest**

327   We wish to confirm that there are no known conflicts of interest associated  
328   with this publication and there has been no significant financial support for  
329   this work that could have influenced its outcome.

## 330   **Acknowledgements**

331   This work was supported in part by the National Science Foundation  
332   under Grant No. CBET-1403403.

## References

- [1] D. O. Lignell, G. C. Fredline, A. D. Lewis, Comparison of one-dimensional turbulence and direct numerical simulations of soot formation and transport in a nonpremixed ethylene jet flame 35 (2) (2015) 1199–1206. doi:10.1016/j.proci.2014.05.046.
- [2] A. W. Abboud, C. Schulz, T. Saad, S. T. Smith, D. D. Harris, D. O. Lignell, A numerical comparison of precipitating turbulent flows between large-eddy simulation and one-dimensional turbulence 61 (10) (2015) 3185–3197. doi:10.1002/aic.14870.
- [3] A. R. Kerstein, One-dimensional turbulence: model formulation and application to homogeneous turbulence, shear flows, and buoyant stratified flows 392 (1999) 277–334. doi:10.1017/S0022112099005376.
- [4] A. R. Kerstein, T. D. Dreeben, Prediction of turbulent free shear flow statistics using a simple stochastic model 12 (2) (2000) 418–424. doi:10.1063/1.870319.
- [5] A. R. Kerstein, W. T. Ashurst, S. Wunsch, V. Nilsen, One-dimensional turbulence: vector formulation and application to free shear flows 447 (2001) 85–109. doi:10.1017/S0022112001005778.
- [6] T. Echekki, A. R. Kerstein, T. D. Dreeben, J.-Y. Chen, ‘one-dimensional turbulence’ simulation of turbulent jet diffusion flames: model formulation and illustrative applications 125 (3) (2001) 1083–1105. doi:10.1016/S0010-2180(01)00228-0.
- [7] J. C. Hewson, A. R. Kerstein, Stochastic simulation of transport and chemical kinetics in turbulent  $\text{co}/\text{h}_2/\text{n}_2$  flames 5 (4) (2001) 669–697. doi:10.1088/1364-7830/5/4/309.
- [8] J. C. Hewson, A. R. Kerstein, Local extinction and reignition in nonpremixed turbulent  $\text{co}/\text{h}_2/\text{n}_2$  jet flames 174 (5-6) (2002) 35–66. doi:10.1080/713713031.
- [9] D. O. Lignell, D. S. Rappleye, One-dimensional-turbulence simulation of flame extinction and reignition in planar ethylene jet flames 159 (9) (2012) 2930–2943. doi:10.1016/j.combustflame.2012.03.018.
- [10] N. Punati, J. C. Sutherland, A. R. Kerstein, E. R. Hawkes, J. H. Chen, An evaluation of the one-dimensional turbulence model: Comparison with direct numerical simulations of  $\text{co}/\text{h}_2$  jets with extinction and reignition 33 (1) (2011) 1515–1522. doi:10.1016/j.proci.2010.06.127.

- [11] A. Abdelsamie, D. O. Lignell, D. Thévenin, Comparison between odt and dns for ignition occurrence in turbulent premixed jet combustion: safety-relevant applications 231 (10) (2017) 1709–1735. doi:10.1515/zpch-2016-0902.
- [12] D. O. Lignell, V. B. Lansinger, A. R. Kerstein, A cylindrical formulation of the one-dimensional turbulence (odt) model for turbulent jet flames, in: AIChE Annual Meeting 2017, American Institute of Chemical Engineers, 2017.
- [13] B. Goshayeshi, J. C. Sutherland, Prediction of oxy-coal flame stand-off using high-fidelity thermochemical models and the one-dimensional turbulence model 35 (3) (2015) 2829–2837. doi:10.1016/j.proci.2014.07.003.
- [14] Z. Jozefik, A. R. Kerstein, H. Schmidt, S. Lyra, H. Kolla, J. H. Chen, One-dimensional turbulence modeling of a turbulent counterflow flame with comparison to dns 162 (8) (2015) 2999–3015. doi:10.1016/j.combustflame.2015.05.010.
- [15] E. I. Monson, D. O. Lignell, M. A. Finney, C. Werner, Z. Jozefik, A. R. Kerstein, R. S. Hintze, Simulation of ethylene wall fires using the spatially-evolving one-dimensional turbulence model 52 (1) (2016) 167–196. doi:10.1007/s10694-014-0441-2.
- [16] J. C. Hewson, A. J. Ricks, S. R. Tieszen, A. R. Kerstein, R. O. Fox, Conditional-moment closure with differential diffusion for soot evolution in fire, in: Center for Turbulence Research, Proceedings of the Summer Program 2006, Stanford University, 2006.
- [17] J. C. Hewson, A. J. Ricks, S. R. Tieszen, A. R. Kerstein, R. O. Fox, On the transport of soot relative to a flame: modeling differential diffusion for soot evolution in fire, in: H. Bockhorn, A. D’Anna, A. F. Sarofim, H. Wang (Eds.), Combustion Generated Fine Carbonaceous Particles, KIT Scientific Publishing, 2009, pp. 571–588.
- [18] D. O. Lignell, J. C. Hewson, One-dimensional turbulence simulation: overview and application to soot formation in nonpremixed flames, in: SIAM Conference on Computational Science and Engineering, 2015.
- [19] A. J. Ricks, J. C. Hewson, A. R. Kerstein, J. P. Gore, S. R. Tieszen, W. T. Ashurst, A spatially developing one-dimensional turbulence (odt) study of soot and enthalpy evolution in meter-scale buoyant turbulent flames 182 (1) (2010) 60–101. doi:10.1080/00102200903297003.

- [20] G. Sun, J. C. Hewson, D. O. Lignell, Evaluation of stochastic particle dispersion modeling in turbulent round jets 89 (2017) 108–122. doi:10.1016/j.ijmultiphaseflow.2016.10.005.
- [21] J. R. Schmidt, J. O. L. Wendt, A. R. Kerstein, Non-equilibrium wall deposition of inertial particles in turbulent flow 137 (2) (2009) 233–257. doi:10.1007/s10955-009-9844-8.
- [22] G. Sun, D. O. Lignell, J. C. Hewson, C. R. Gin, Particle dispersion in homogeneous turbulence using the one-dimensional turbulence model 26 (10) (2014) 103301. doi:10.1063/1.4896555.
- [23] M. Fistler, D. O. Lignell, A. R. Kerstein, M. Oevermann, Numerical studies of turbulent particle-laden jets using spatial approach of one-dimensional turbulence, in: ILASS-Europe 28th Conference on Liquid Atomization and Spray Systems, 2017.
- [24] S. Cao, T. Echekki, A low-dimensional stochastic closure model for combustion large-eddy simulation 9. doi:10.1080/14685240701790714.
- [25] R. C. Schmidt, A. R. Kerstein, S. Wunsch, V. Nilsen, Near-wall les closure based on one-dimensional turbulence modeling 186 (1) (2003) 317–355. doi:10.1016/S0021-9991(03)00071-8.
- [26] R. C. Schmidt, A. R. Kerstein, R. McDermott, Odtles: A multi-scale model for 3d turbulent flow based on one-dimensional turbulence modeling 199 (13-16) (2010) 865–880. doi:10.1016/j.cma.2008.05.028.
- [27] E. Gonzalez-Juez, A. R. Kerstein, D. O. Lignell, Fluxes across double-diffusive interfaces: a one-dimensional-turbulence study 677 (2011) 218–254. doi:10.1017/jfm.2011.78.
- [28] E. Gonzalez-Juez, A. R. Kerstein, D. O. Lignell, Reactive rayleigh–taylor turbulent mixing: a one-dimensional-turbulence study 107 (5) (2013) 506–525. doi:10.1080/03091929.2012.736504.
- [29] S. Wunsch, A. R. Kerstein, A model for layer formation in stably stratified turbulence 13 (3) (2001) 702–712. doi:10.1063/1.1344182.
- [30] D. O. Lignell, V. B. Lansinger, J. Medina, M. Klein, A. R. Kerstein, H. Schmidt, M. Fistler, M. Oevermann, One-dimensional turbulence modeling for cylindrical and spherical flows: model formulation and application 32 (4) (2018) 495–520. doi:10.1007/s00162-018-0465-1.



- [31] M. Klein, D. O. Lignell, H. Schmidt, Map-based modeling of turbulent convection: Application of the one-dimensional turbulence model to planar and spherical geometries, in: International Conference on Rayleigh-Benard Turbulence, 2018.
- [32] M. Klein, D. O. Lignell, H. Schmidt, Stochastic modeling of temperature and velocity statistics in spherical-shell convection, in: EGU Conference on Recent developments in Geophysical Fluid Dynamics, 2019.
- [33] W. T. Ashurst, A. R. Kerstein, One-dimensional turbulence: Variable-density formulation and application to mixing layers 17 (2). doi:10.1063/1.1847413.
- [34] D. O. Lignell, A. R. Kerstein, G. Sun, E. I. Monson, Mesh adaption for efficient multiscale implementation of one-dimensional turbulence 27 (3-4) (2013) 273–295. doi:10.1007/s00162-012-0267-9.
- [35] Y. A. Çengel, J. M. Cimbala, Fluid Mechanics, 2nd Edition, Çengel series in engineering thermal-fluid sciences, McGraw-Hill Higher Education, 2010.
- [36] J. Beder, yaml-cpp v0.6.3 (2008).  
URL <https://github.com/jbeder/yaml-cpp/>
- [37] A. C. Hindmarsh, R. Serban, D. R. Reynolds, CVODE, [https://computing.llnl.gov/sites/default/files/public/cv\\_guide.pdf](https://computing.llnl.gov/sites/default/files/public/cv_guide.pdf) (2020).  
URL <https://computing.llnl.gov/projects/sundials/cvode>
- [38] G. Strang, On the construction and comparison of difference schemes 5 (3) (1968) 506–517. doi:10.1137/0705041.
- [39] D. G. Goodwin, R. L. Speth, H. K. Moffat, B. W. Weber, Cantera (2018). doi:10.5281/zenodo.1174508.  
URL <https://cantera.org/>
- [40] D. van Heesch, Doxygen (2018).  
URL <https://www.doxygen.nl/>
- [41] A. B. Yoo, M. A. Jette, M. Grondona, Slurm: simple linux utility for resource management, in: D. G. Feitelson, L. Rudolph, U. Schwiegelshohn (Eds.), Job Scheduling Strategies For Parallel Processing, Vol. 2862 of Lecture notes in computer science, 0302-9743, Springer, 2003, pp. 44–60. doi:10.1007/10968987-3.

- [42] W. Meier, R. S. Barlow, Y.-L. Chen, J.-Y. Chen, Raman/Rayleigh/LIF measurements in a turbulent  $\text{CH}_4/\text{H}_2/\text{N}_2$  jet diffusion flame: experimental techniques and turbulence–chemistry interaction 123 (3) (2000) 326–343. doi:10.1016/S0010-2180(00)00171-1.  
URL <https://tnfworkshop.org/data-archives/simplejet/dlrflames/>
- [43] H. Pitsch, Unsteady flamelet modeling of differential diffusion in turbulent jet diffusion flames 123 (3) (2000) 358–374. doi:10.1016/S0010-2180(00)00135-8.
- [44] R. P. Lindstedt, H. Ozarovsky, Joint scalar transported pdf modeling of nonpiloted turbulent diffusion flames 143 (4) (2005) 471–490. doi:10.1016/j.combustflame.2005.08.030.
- [45] H. Wang, S. B. Pope, Large eddy simulation/probability density function modeling of a turbulent  $\text{CH}_4/\text{H}_2/\text{N}_2$  jet flame 33 (1) (2011) 1319–1330. doi:10.1016/j.proci.2010.08.004.
- [46] M. Fairweather, R. M. Woolley, First-order conditional moment closure modeling of turbulent, nonpremixed methane flames 138 (1-2) (2004) 3–19. doi:10.1016/j.combustflame.2004.03.001.
- [47] K. W. Lee, D. H. Choi, Prediction of  $\text{NO}$  in turbulent diffusion flames using eulerian particle flamelet model 12 (5) (2008) 905–927. doi:10.1080/13647830802094351.
- [48] K. W. Lee, D. H. Choi, Analysis of  $\text{NO}$  formation in high temperature diluted air combustion in a coaxial jet flame using an unsteady flamelet model 52 (5-6) (2009) 1412–1420. doi:10.1016/j.ijheatmasstransfer.2008.08.015.

#### Current executable software version

Ancillary data table required for sub version of the executable software: (x.1, x.2 etc.) kindly replace examples in right column with the correct information about your executables, and leave the left column as it is.

Nr.	(Executable) software meta-data description	Please fill in this column
S1	Current software version	2.1
S2	Permanent link to executables of this version	For example: <i>https</i> : <i>//github.com/combogenomics/DuctApe/releases/tag/DuctApe-0.16.4</i>
S3	Legal Software License	MIT
S4	Computing platforms/Operating Systems	Linux, OS X, Microsoft Windows
S5	Installation requirements & dependencies	CMake 3.12+, Cantera, Git, Doxygen (optional)
S6	If available, link to user manual - if formally published include a reference to the publication in the reference list	For example: <i>http</i> : <i>//mozart.github.io/documentation/</i>
S7	Support email for questions	davidlignell@byu.edu

Table 2: Software metadata (optional)